Materials and Design 31 (2010) 4800–4807

Contents lists available at ScienceDirect

Materials and Design

journal homepage: www.elsevier.com/locate/matdes

Joining of CP-Ti to 304 stainless steel using friction stir welding technique

M. Fazel-Najafabadi, S.F. Kashani-Bozorg *, A. Zarei-Hanzaki

School of Metallurgy and Materials Engineering, University College of Engineering, University of Tehran, P.O. Box 11155-4563, Tehran, Iran

ARTICLE INFO

Article history:
Received 16 October 2009
Accepted 1 May 2010
Available online 8 May 2010

Keywords:
Welding
Mechanical
Microstructure

ABSTRACT

Friction stir welding parameters were adjusted in order to achieve defect-free dissimilar lap joint of CP-Ti to 304 stainless steel. Titanium as a softer material was selected to be on the lap top side. The joint stir zone was found to be consisted of two main regions; the dominant fine dynamically re-crystallized titanium grains at the upper region and a minor composite-type microstructure of fragments of 304 stainless steel in a matrix of fine dynamically re-crystallized titanium grains in the lower region. The stir zone was separated from the 304 stainless steel side by an interface layer of TiFe-based crystal structure. Joint shear strength was measured; a maximum failure load of ~73% of that of CP-Ti was achieved. This was associated with the occurrence of fracture at the joint intermetallic-based interface. The failure load value of the fabricated joints is related to the thickness of the intermetallic interface.

© 2010 Elsevier Ltd. All rights reserved.

1. Introduction

Dissimilar joints can provide weight/cost savings due to less usage of one of the components. In addition, they are capable of offering complex function in engineering applications. Joining between commercial pure titanium (CP-Ti) and 304 stainless steel (304 SS) is considered in power plant industries. Previously, fusion welding joints between CP-Ti and 304 SS exhibited poor mechanical properties due to the formation of brittle intermetallic phases and titanium oxides at the interface [1,2]. Also, other joining methods were examined such as brazing [3–5] and diffusion bonding [6,7]. For example, Yue et al. reported brazing of titanium alloy to 304 SS using an AgCuTi filer metal [3]. It was shown that formation of brittle intermetallic phase decreased the joint shear strength to a value lower than that of titanium alloy. In another investigation it was found that using (Ni)/Cr barrier layer increased the shear strength of the brazed joint of titanium to 304 SS [4]. Relatively better results were reported on the usage of diffusion bonding technique. However, there are limitations related to shape and geometry of specimens [6,7]. In summary, solid state bonding technique can be more suitable than those related to fusion ones since many problems associated with melting are eliminated or reduced.

Friction stir welding (FSW) is an innovative solid state bonding technique. In early years, it was introduced for light alloys. Recently, high performance tool materials are employed for FSW of high melting temperature materials such as titanium, nickel and steels [8,9]. In addition, satisfactory dissimilar joints of Al/Mg [10], Al/Cu [11], and Al/304 SS [12] were achieved using FSW technique. When FSW is used to join dissimilar materials, it is not easy to produce sound joints due their different deformation characteristics under the rotating and advancing tool material [8]. It was reported that a better FSW configuration was acquired when the welding tool was essentially plunged into the softer material [13]. Chen and Nakata studied the microstructural characterization and mechanical properties of friction stir welded joint between pure titanium and Al–Si alloy: a $TiAl_3$ intermetallic phase was found at the joint interface and a maximum joint failure load of ~62% of that of Al was achieved. The joints were fractured at the interface of two materials [14]. Uzun et al. studied FSW of Al/304 SS couple; diffusion of Al to the 304 SS side was observed, however no intermetallic phase was detected at the joint interface [12]. Watanabe et al. studied FSW of Al/steel couple. They reported a maximum joint strength of ~280 MPa. Also, FeAl and $FeAl_3$ intermetallic phases were detected at the joint interface [13].

FSW of dissimilar CP-Ti/SS couple has not been reported in the literature. However, successful similar joining of each alloy was reported; Lee et al. [14], Zhang et al. [15], Mironov et al. [16] and Fujii et al. [17] used a sintered TiC, a polycrystalline cubic boron nitride, a Mo-based alloy, and a tungsten carbide based alloy tools for FSW of pure titanium, respectively. Also, austenitic stainless steel plates were friction stir welded by Sato et al. [18] using a cubic boron nitride tool. Hard tool materials were selected for FSW of these high strength alloys since tool worn-out is a major problem, which can hinder commercialization of this technique for high strength materials. However, when considering dissimilar joint, since the conventional fusion techniques are associated with solidification problems, usually joint with adequate mechanical properties cannot be achieved. In these cases, FSW can be considered as a candidate process since joining is done in the absence of liquid phase transition.

* Corresponding author. Tel.: +98 21 82084105; fax: +98 21 88006076.
E-mail address: fkashani@ut.ac.ir (S.F. Kashani-Bozorg).

0261-3069/$ - see front matter © 2010 Elsevier Ltd. All rights reserved.
doi:10.1016/j.matdes.2010.05.003

In the present investigation, the effects of FSW process parameters were investigated on producing defect-free dissimilar CP-Ti/SS lap joints. Joint microstructures and its associated zones were characterized. In addition, assessment of dissimilar joint shear strength was presented. Lap joining mechanism of titanium/stainless steel using friction stir welding technique was systematically discussed.

2. Experimental procedure

The materials used in the present investigation were plates of CP-Ti and 304 stainless steel (each with a thickness of 4 mm). Tables 1 and 2 show the nominal chemical compositions of the as-received materials. Rectangular pieces with a length and width of 100 and 50 mm were cut and cleaned in an ultra sonic bath, respectively. A conventional miller machine was employed for the welding experiments. A tungsten carbide tool was used with a shoulder and pin diameter of 28 and 8 mm, respectively. The pin length was about 2.5 mm. The tool was operated with a back tilt of 2°.

Pieces of CP-Ti and 304 SS plates were placed on a traveling table according to Fig. 1. A lap joint design was selected; titanium was placed over stainless steel plate. Welding parameters were tool rotation speeds of 560, 710, 900 and 1100 rpm and tool advancing speeds of 25, 40, 50 and 80 mm/min. The stir zone temperature was measured just as passed by the tool using a portable infrared thermometer model Raytek 3i. Also, a K-type thermocouple was inserted between CP-Ti/SS plates in their middle length (5 mm far from either side of the plates. The temperature was recorded as a function of time.

The dissimilar joints were cross-sectioned perpendicular to the welding direction for metallographic analyses and tensile tests using an electrical-discharge cutting machine. Cross-sections of the dissimilar joints were mechanically ground down with SiC abrasive papers and then polished on a cloth using 0.05 μm alumina paste. Microstructure was studied using optical and scanning electron microscopes (SEM). Elemental distribution at the joint interface was detected by energy dispersive X-ray spectrometer (EDS) system that was linked with the SEM. The crystal structure of joints surface and interface were analyzed using X-ray diffraction (XRD). Inspection of the lap joints was carried out using an X-ray fluoroscope model MU41. The joints shear strength value was evaluated at room temperature using an AT250 tensile testing machine. Three rectangular tensile specimens with a width of 15 mm were prepared and examined from each welded pieces.

Table 1
Nominal chemical composition of the as-received CP-Ti (wt.%).

Element	Fe	O	N	C	H	Ti
wt.%	0.04	0.06	0.003	0.007	0.004	Balance

Table 2
Nominal chemical composition of the as-received 304 SS (wt.%).

Element	Mn	Si	Cr	Ni	Mo	Cu	Ti	C	Fe
wt.%	0.94	0.31	18.2	8.3	0.14	0.03	0.01	0.022	Balance

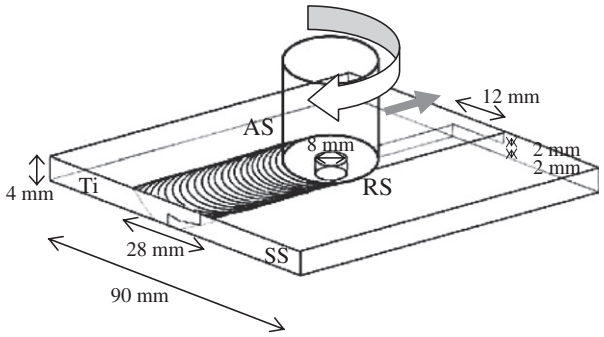

Fig. 1. Schematic diagram of the geometry of a dissimilar CP-Ti/304 SS lap design.

3. Results and discussion

3.1. Effects of FSW process parameters

No sound joint was resulted using the lowest applied rotation speed (560 rpm, Fig. 2a). Many voids in the length of the track were observed. The generated heat input at a rotation speed of 560 rpm was not enough to provide sufficient plasticity and flow of materials within the weld nugget. Thus, the rotation speed was increased to generate greater heat inputs. Top views of the processed materials using the relatively higher rotation speed of 710 rpm exhibited the formation of a weld track with shiny metallic color and acceptable appearance (Fig. 2b). This can be attributed to the achievement of higher local temperatures, which provided sufficient plasticity of materials. In this case, the associated materials flow can give rise to direct contacts between CP-Ti and 304 SS to form a dissimilar joint. However, increasing the rotation speed to 900 rpm was resulted in weld appearance with slight transition from yellow to blue color. Further increasing the rotation speed (to 1100 rpm) produced a non-uniform weld with dark appearance. This is an indication of partial oxidation of titanium. It is noticeable that higher nugget temperature associated with higher rotation speed can increase the chance of oxygen pick-up by titanium. Titanium is a reactive metal at high temperature in the ambient atmosphere. Although the process was conducted under the argon shielding gas, however substantial oxygen was picked up. This scenario is consistent with changing the surface appearance from metallic to yellow, blue and dark by increasing the tool rotation speed. Also, this is supported by EDS analysis (Fig. 3)

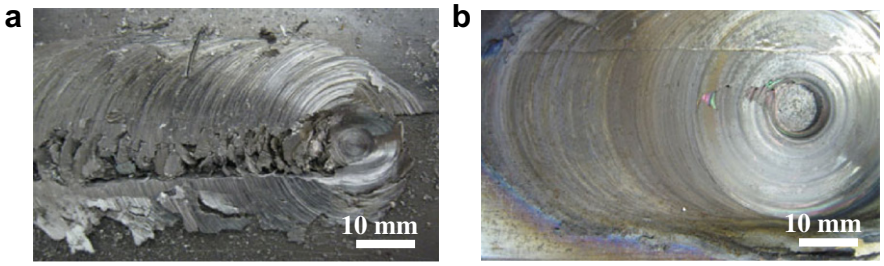

Fig. 2. Top views of dissimilar CP-Ti/304 SS lap welding using a fixed tool advancing speed of 25 mm/min and various tool rotating speeds, (a) 560 rpm, (b) 710 rpm.

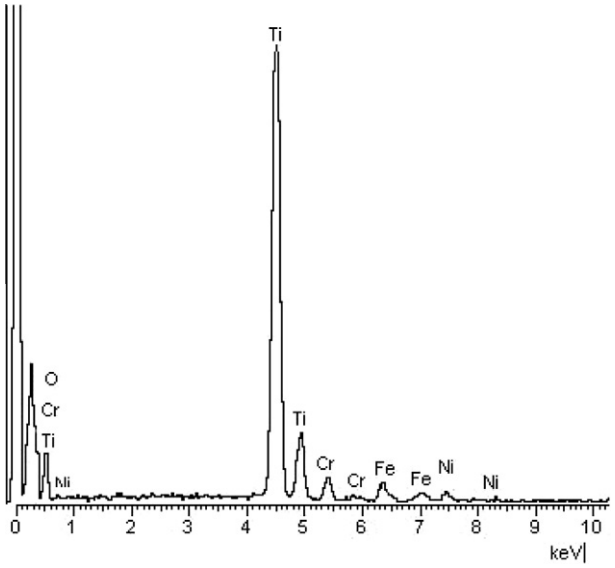

Fig. 3. Energy dispersive spectrum of the top view of the lap joint produced using the rotation and advancing speeds of 1100 rpm and 25 mm/s, respectively showing substantial oxygen picked up.

which showed substantial oxygen in the joint produced using the highest heat input (the highest rate of rotation/advancing speed), however no TiO_2 was detected by XRD which presumed to be related to its low volume fraction. Solid solution of oxygen in titanium and formation of oxide films or particles can decrease the titanium plasticity and its flow, which deteriorates the stir zone and prevents direct contact of titanium with 304 SS.

On the other hand, employing a relatively high advancing speed of 80 mm/s was resulted in the formation of partial joint with severe tunnel defects. In fact, a higher advancing speed brings lower heat input at each tool location; this is associated with relatively lower nugget temperature, inadequate materials plasticity, low flow rate of material and lack of direct contact between CP-Ti and 304 SS. Furthermore, imperfect joint with no mechanical mixing of CP-Ti and 304 SS was resulted.

In general, joints with sound appearance were achieved using tool rotation and advancing speeds in the ranges of 700–1100 rpm and 25–50 mm/min, respectively. These parameters are not consistent with those reported for similar joint of CP-Ti plates [14]. The need of higher heat input for the adequate plasticity of 304 SS material is believed to be responsible for the usage of relatively lower tool advancing speed.

3.2. The joint microstructure and its associated regions

A typical cross-section of the friction stir lap welded track with sound appearance is shown in Fig. 4. It presents various regions with different microstructures; a thin layer of interface between the stir zone and 304 SS side, a stir zone (SZ) along the weld center line, a thermo-mechanically affected zone (TMAZ) and a heat-affected zone (HAZ) on each sides of the weld.

A maximum temperature of ~1350 K was measured by external thermometer and internal thermocouple (Fig. 5), thus considering their associated time lags, the actual temperature of the stir zone is expected to be substantial beyond 1350 K; this temperature provided elemental diffusion across the SZ/304 SS boundary which resulted in the formation of a thin layer of TiFe-based intermetallic compound as a joint interface (Fig. 6a). The EDS point analysis results suggest that TiFe-based intermetallic compound was formed at the interface of SZ/304 SS side (Fig. 6b). In addition, reflections related to this crystal structure were found in the X-ray diffraction pattern of the joint fractured surface (Fig. 7). Formation of intermetallic interface was previously reported in other solid-state welding methods [19,20]. The increase of elemental migrations across the interface due to increment of temperature provides reaction between Ti and Fe and formation of TiFe-based intermetallic phase.

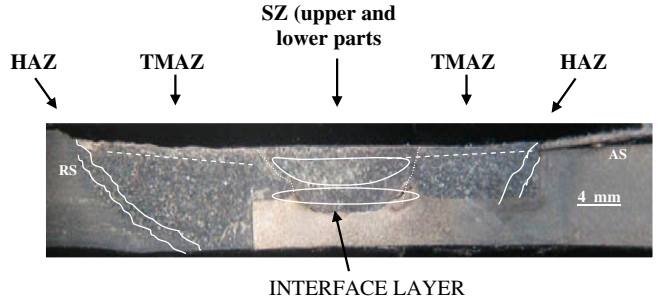

Fig. 4. Cross-section of a typical CP-Ti/304 SS lap welded plates exhibiting various regions.

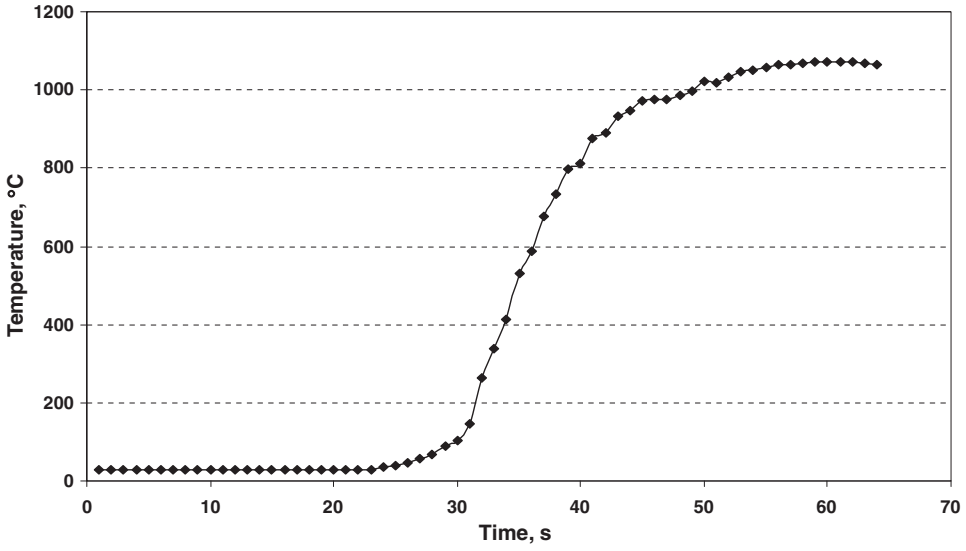

Fig. 5. The temperature of CP-Ti/304 SS interface measured (at middle of the plates, i.e. 5 cm from each side) as a function of time using a tool rotation and advancing speed of 1100 rpm and 50 mm/s, respectively.

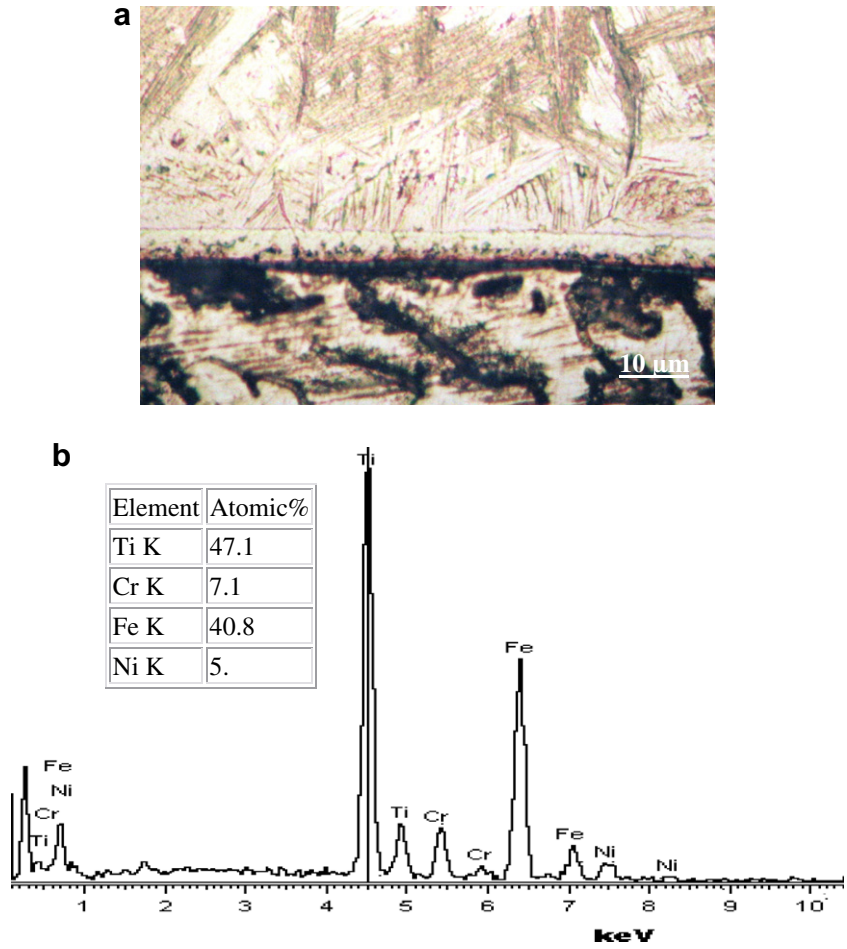

Fig. 6. Interface layer at the lap joint of CP-Ti/304 SS joint, (a) optical micrograph, (b) energy dispersive spectrum.

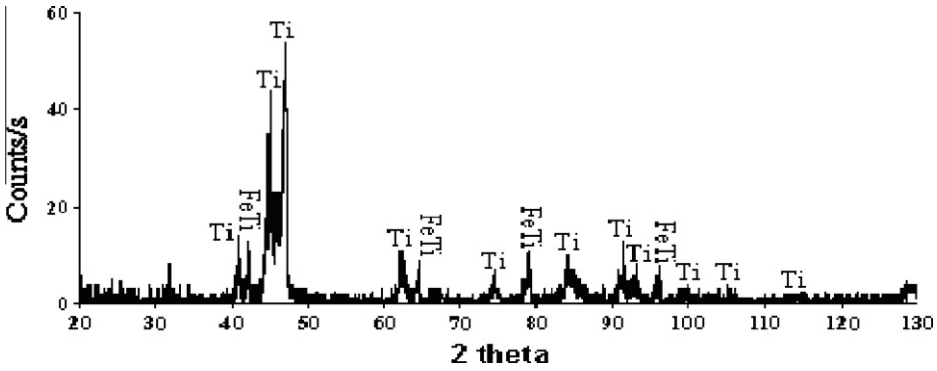

Fig. 7. XRD spectrum of Ti side of a fractured joint showed extra reflection related to TiFe intermetallic compound.

Binary phase diagram of Ti and Fe shows two intermetallic compounds, TiFe and $TiFe_2$ [19]. However, XRD and EDS results are consistent with TiFe-based crystal structure; this is in agreement with thermodynamic calculations, which show that TiFe has the lower free energy of formation than $TiFe_2$ compound [19]. Thus, it is understandable that in the reaction of Ti and Fe during FSW, TiFe phase forms at the interface preferentially. The thickness of the intermetallic layer was found to be ~3 μm in the joint produced using the tool rotation and advancing speeds of 1100 rpm and 50 mm/s, respectively (Fig. 6a). The joint interface thickness was found to increase with increasing tool rotating/advancing speed ratio. Lee et al. [21] detected an intermetallic (Al_4Fe) layer with a thickness of ~250 nm in dissimilar welding of Al/304 SS using FSW. However, a relatively thicker layer is usually formed in diffusion bonding of dissimilar joints [21]. A TiFe-based layer with a thickness of ~6 μm was found in diffusion bonding of CP-Ti to 304 SS using the lowest applied time and temperature [20]. In FSW technique, since the high temperature dwell time of the SZ is relatively short, diffusion is limited, thus thinner interface layer expected.

Fig. 4 shows that the pin was penetrated in part of 304 SS plate. Substantial 304 SS material was fragmented by the rotating pin tool and taken to the titanium side (Fig. 8). This created a composite-type structure of titanium matrix reinforced by 304 SS fragments (detected by EDS) at the SZ near the SZ/304 SS boundary (Fig. 8). These fragments were appeared with lenticular/irregular

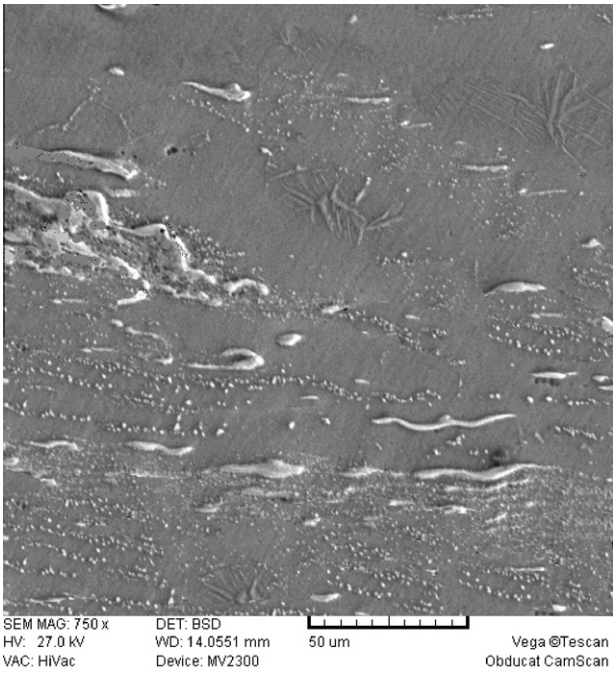

Fig. 8. A composite-type microstructure at the lower part of the SZ showing 304 SS fragments in a matrix of titanium.

shapes and found to be aligned in the local flow directions within the center of the SZ close to 304 SS boundary.

The dominant part of the SZ was found to be in its center and up to the top of weld nugget. This region showed a microstructure of fine equiaxed titanium grains (Fig. 9). In FSW, the pin tool into the SZ material [12] imposes both frictional heat and severe plastic deformation. In this experiment, as the SZ temperature was measured to be well higher than of the α-Ti $\rightarrow$ β-Ti transus temperature (Fig. 5); thus, the titanium was hot deformed in the β crystal structure state. The fine grains of the SZ in comparison to those of the unaffected CP-Ti substrate, reflects the occurrence of a dynamic recrystallization process [15]. These fine equiaxed grains are prior β grain. After passage of the tool, the β-Ti structure transforms to α-Ti during the cooling stage of the FSW process. In this experiment, the rate of cooling was not measured since the tool pin cut off the thermocouple tip. However, relatively high cooling rate is expected for the FSW process due to the heat sink effect of the plates. The prior β-Ti re-crystallized grains showed substructure; this is suggested to be formed during cooling stage.

The SZ grains exhibited lens- and wedge-shaped twins and subgrain boundary features. These substructural features are not consistent with body centered cubic structure of the β-Ti. Lee et al. [14] investigated the friction stir zone of pure titanium and detected a grainy microstructure with a large amount of twin structure along with thick dislocation wall and dislocation tangles using transmission electron microscopy. The production of these features was presumed to be related to plastic deformation and frictional heat; slip system is limited in hexagonal packed structure of titanium, thus twinning mode is involved even at low strains. The generated dislocations due to slip mode are dissociated into partials and planar arrays of stacking faults in the hexagonal close packed structure of the α-Ti with low stacking fault energy. This develops fine twinning substructure.

The transformation of β-Ti $\rightarrow$ α'-Ti on rapid cooling is well documented. However, the present investigation showed that actual deformation of the SZ was done at the high temperature β-Ti phase field due to tool rotation and advancing action. The X-ray diffraction pattern of the SZ was consistent with α-Ti crystal structure however; the reflection showed substantial peak broadening (Fig. 7). This is not related to crystallite size referring to the ob-

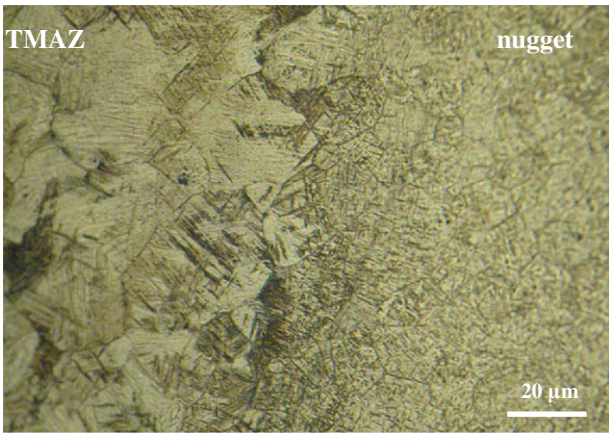

Fig. 10. Transition of SZ to TMAZ microstructure showing deformation substructure of relatively larger grain of the former.

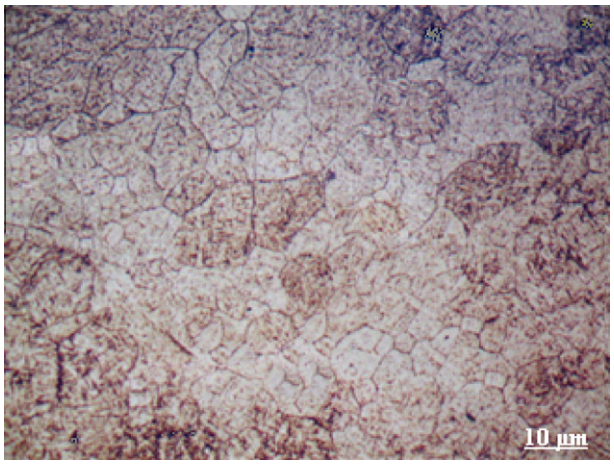

Fig. 9. Microstructure of the center SZ exhibiting fine dynamically re-crystallized prior β-Ti grains.

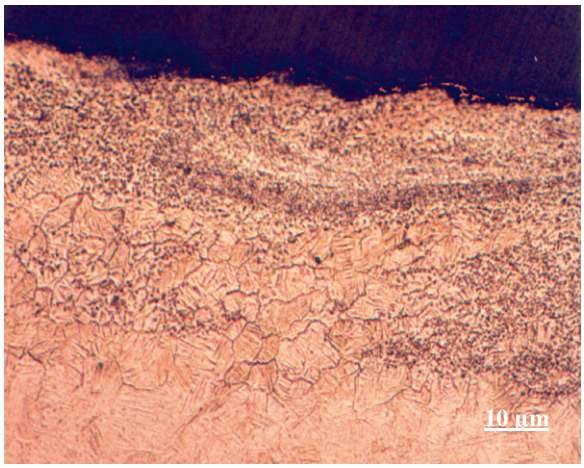

Fig. 11. The HAZ microstructure exhibiting grain growth and serrated grain boundary and fine twin substructure at the top of SZ.

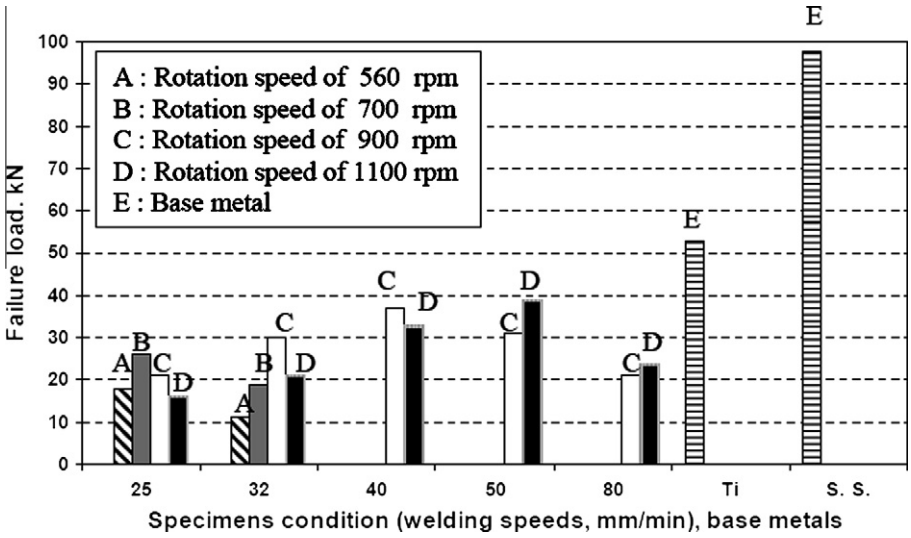

Fig. 12. Failure loads of dissimilar CP-Ti/SS lap joints produced using different FSW process parameters.

served microstructure. On the other hand, the peak broadening should be related the strain associated with thermal stress, which appears upon cooling the SZ; these are believed to be responsible for deformation features in α phase, which is formed after pin tool passage at relatively lower temperature.

The grain boundaries at the region near the top surface of the SZ were not resolved. Zhang et al. reported of fine lath-shaped grains in this region [15]. Fig. 11 exhibits these fine features; however, it is believed that they are grain substructure. It should be born in mind that this region experienced forging due to the slightly inserted rotating tool. Thus, the re-crystallized grain showed finer lath/twin-shaped feature.

Away from the SZ, on the both sides, a narrow transition region was observed (Fig. 10). The titanium grain was found to be coarser than those of the SZ were. In addition, the grains exhibited wedge shape twin/lath-type martensite features. This region is believed to be thermo-mechanically affected zone (TMAZ) since experienced thermal (due to grain growth) and mechanical (because of strain related substructure) cycles. Such region appears as elongated grain in aluminium alloys [8]. However, titanium is classified as low stacking fault metals with limited slip system (contrary to aluminium); this promotes stacking faults and bands of deformation twins. Twinning occur to accommodate the strain induced by the pin tool and better align the lattice with the shear. Lee et al. [14] and Zhang et al. [15] did not observe TMAZ in the friction stir weld of titanium. Also, Knipling and Fonda [22] found no apparent TMAZ in the FSW of near α-titanium alloy. Resolving TMAZ is believed to be difficult due to its narrowness and limited grain elongation.

Away from the TMAZ, and adjacent to the unaffected substrate grains, region of coarser grains were observed (Fig. 11). These grains experienced thermal cycle, so it is named heat-affected zone (HAZ). Serrated grain boundaries were observed in this region. The interrupted grain boundaries can be related to phase transformation upon cooling from the high temperature β phase.

3.3. Joint mechanical properties

The joints with sound appearance were selected after visual inspection and microscopic examination of cross-section. The selected joints showed no clear defect by fluoroscopy. The tensile test results of the welded specimens are shown in Fig. 12. The failure loads of all joints were found to be lower than those of the base materials. The shear specimen of all lap joints were fractured at the interface of SZ/SS side (Fig. 13a and b), however at regions near the end side of the joint, rupturing was found to be within the stir zone (Fig. 13a and b). In general, observation of the fractured parts by the naked eye showed nearly flat surface with bright contrast and chevron marks similar to those produced on the titanium surface by the tool rotation and travel.

Further investigation of the fractured surface by scanning electron microscope is depicted in Fig. 14. A river pattern is observed on both fractured surface (Fig. 14) reflecting of a cleavage type transgranular fracture. EDS analyses of the fractured surfaces were consistent with TiFe-based structure.

Higher failure load was resulted employing a tool rotation and advancing speeds of 900–1100 rpm and 40–50 mm/min, respectively. (The maximum failure load of 39 kN was measured for the joint produced using a tool rotation and advancing speeds of 1100 rpm and 50 mm/min, respectively.) The measured failure load value at a fix rotation speed of 1100 rpm shows decreasing using advancing speeds of 25, 32 and 80 mm/min. In the case of lower advancing speeds of 25 and 32 mm/min, the decrease in failure load value is attributed mainly to greater heat input, which thickened the TiFe interface layer. In addition, higher oxygen pick-up by titanium and possible formation of oxide film prevents direct contact of titanium with stainless steel and lower the joint failure load. Moreover, thicker intermetallic interface can involve longer distance migration of elements; this may be associated with more Kirkendall voids that lower joint failure load. Other research-

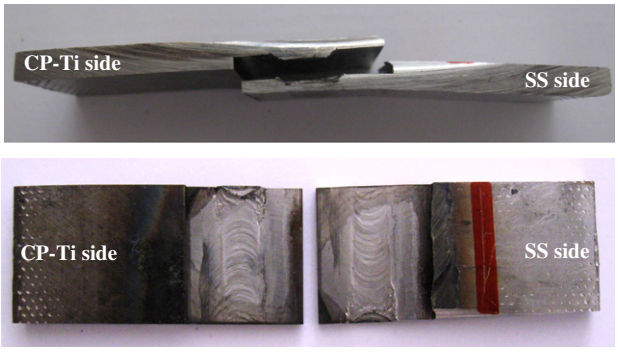

Fig. 13. Fractured parts of the lap joint of CP-Ti/304 SS produced using tool rotation and advancing speeds of 1100 rpm and 50 mm/s, respectively. The fracture occurred at the interface layer, (a) cross view, (b) top view.

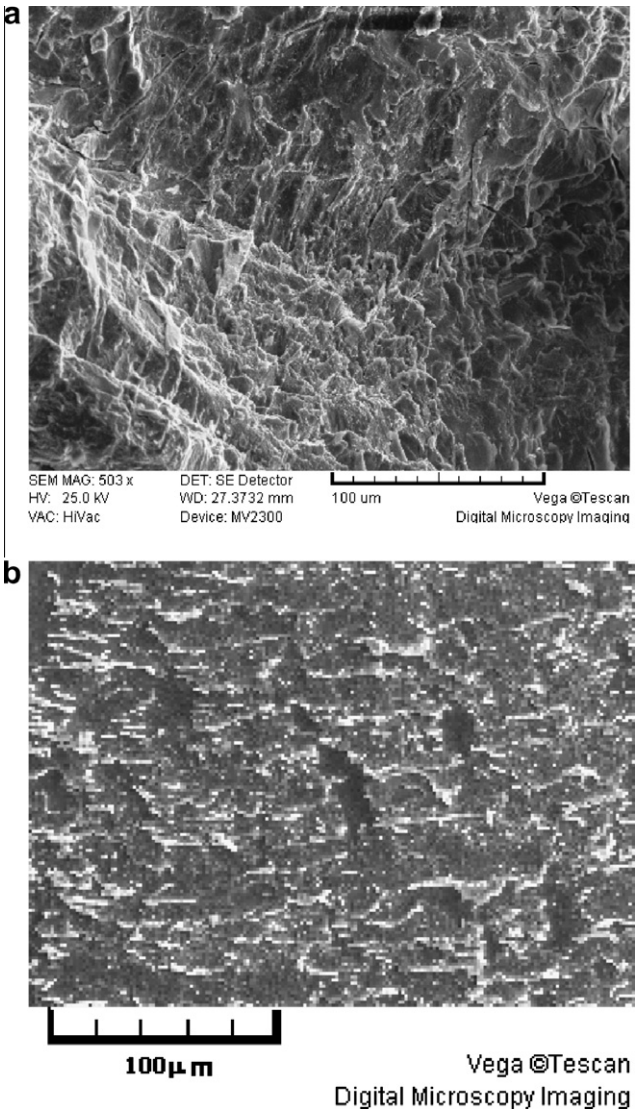

Fig. 14. Fractured surfaces of lap joint of dissimilar CP-Ti/304 SS produced using tool rotation and advancing speeds of 1100 rpm and 50 mm/s, respectively, (a) CP-Ti side and (b) 304 SS side, both exhibiting of river pattern which reflects of a brittle transgranular fracture.

ers reported the formation of intermetallic interface and its dominant role on joint mechanical properties in FSW; Fuji et al. who showed that the dominant factor determining the joint mechanical characteristic in friction welds of Al to Ti was the thickness of the $TiAl_3$ intermetallic compound layer produced at the interface. They found that the critical thickness of the intermetallic compound layer was about 5 μm [23]. In addition, a thin layer of $TiAl_3$ was found at the interface of friction stir lap welded Ti and Al [24].

The lower failure load of the joint produced using lower heat input (advancing speed of 80 mm/min) is associated with formation of a very thin interface. Thus, it can be concluded that the key factor of a sound dissimilar joint of CP-Ti/SS can be achieved thru controlling the thickness of the TiFe-based intermetallic layer, which is formed at the stir zone/SS interface by adjusting the FSW process parameters. In addition, ambient protection is highly recommended.

The test results show no evidence of either inadequate strength of the SZ composite-type region or insufficient adhesion of SS particles to titanium at the lower part of the SZ.

Two joint mechanisms are involved; the chemical bonding at the interface with the formation of TiFe-based intermetallic compound and mechanical reinforcement of dispersion of SS fragments in the titanium matrix at the lower part of the SZ.

The sequence of joining mechanism is proposed to be as follows:

In the beginning, the material under the tool undergoes the synthetic effect of thermal and mechanical cycle. Thus, relatively high temperature and severe pressure are generated. High pressure results in the rupture of surface oxide films of both materials, which causes intimate contact between titanium and stainless steel.

Then, the generated heat by FSW raises the temperature to initiate the following reaction [19]:

$$\mathrm{Ti} + \mathrm{Fe} \rightarrow \mathrm{TiFe} + \mathrm{Heat} \quad (1)$$

The released heat increases temperature, which promotes the reaction.

Finally, TiFe phase remains the only reaction product at the CP-Ti/SS interface.

In lap joining using FSW, when the tool is inserted into the underside stainless steel, its fragments are taken to the upper titanium side in a complex vortex-type pattern. Due to pin stirring action, relatively softer titanium is extruded between the stainless steel fragments. The stainless steel fragments are distributed within the recrystallised titanium matrix.

4. Conclusions

In summary, the following conclusions are reached:

1. Sound dissimilar lap joint of CP-Ti/304 SS was achieved employing FSW technique by adjusting tool rotation and advancing speeds under the protecting atmosphere.
2. The stir zone consists of the dominant dynamically re-crystallized fine titanium grain at the center and upper part and a composite-type structure of stainless steel fragments in a matrix of fine titanium grains.
3. An intermetallic TiFe-based layer was found at the stir zone/stainless steel boundary with a thickness, which increases with increasing tool rotation/advancing speeds rate.
4. Lap joint with a maximum failure load of 73% of that of CP-Ti was achieved by adjusting tool rotation and advancing speeds.

Acknowledgement

Partial financial support from University of Tehran (No. 810713/6/17) is gratefully acknowledged.

References

[1] Akhter JI, Ahmad M, Ali G. Diffusion bonding of Ti coated Zircaloy-4 and 316-L stainless steel. Mater Charact 2009;60:193–6.
[2] Kang BY, Prasada Yarlagadda KDV, Kang MJ, Kim HJ, Kim IS. The effect of alternate supply of shielding gases in austenite stainless steel GTA welding. J Mater Process Technol 2009;209:4722–7.
[3] Yue X, He P, Feng JC, Zhang JH, Zhu FQ. Microstructure and interfacial reactions of vacuum brazing titanium alloy to stainless steel using an AgCuTi filler metal. Mater Charact 2008;59:1721–7.
[4] Shiue RK, Wu SK, Shiue JY. Infrared brazing of Ti–6Al–4V and 17–4 PH stainless steel with (Ni)/Cr barrier layer(s). Mater Sci Eng A 2008;488:186–94.
[5] Elrefaey A, Tillmann W. Effect of brazing parameters on microstructure and mechanical properties of titanium joints. J Mater Process Technol 2009;209:4842–9.
[6] Atasoy Evren E, Kahraman N. Diffusion bonding of commercially pure titanium to low carbon steel using a silver interlayer. Mater Charact 2008;59:1481–90.
[7] Elrefaey A, Tillmann W. Solid state diffusion bonding of titanium to steel using a copper base alloy as interlayer. J Mater Process Technol 2009;209:2746–52.
[8] Mishra RS, Ma ZY. Friction stir welding and processing. Mater Sci Eng R 2005;50:1–78.

[9] Nandan R, Debroy T, Bhadeshia B. Recent advances in friction-stir welding-process, weldment structure and properties. Prog Mater Sci 2008;53:980.
[10] Chen YC, Nakata K. Friction stir lap joining aluminum and magnesium alloys. Scr Mater 2008;58:433–6.
[11] Ouyang J, Yarrapareddy E, Kovaceric R. Microstructural evolution in the friction stir welded 6061 aluminum alloy (T6-temper condition) to copper. J Mater Process Technol 2006;172:110–22.
[12] Uzun H, Donne CD, Argagnotto A, Ghidini T, Gambaro C. Friction stir welding of dissimilar Al 6013–T4 to X5CrNi18–10 stainless steel. Mater Des 2005;26:41–6.
[13] Watanabe T, Takayama H, Yanagisawa A. Joining of aluminum alloy to steel by friction stir welding. J Mater Process Technol 2006;178:342–9.
[14] Lee WB, Lee CY, Chang WS, Yeon YM, Jung SB. Microstructural investigation of friction stir welded pure titanium. Mater Lett 2005;59:3315–8.
[15] Zhang YU, Sato YS, Kokawa H, Park SHC, Hirano S. Stir zone microstructure of commercial purity titanium friction stir welded using pcBN tool. Mater Sci Eng A 2008;488:25–30.
[16] Mironov S, Sato YS, Kokawa H. Development of grain structure during friction stir welding of pure titanium. Acta Mater 2009;57:4519–28.
[17] Fujii H, Sun Y, Kato H, Nakata K. Investigation of welding parameter dependent microstructure and mechanical properties in friction stir welded pure Ti joints. Mater Sci Eng A 2010;527:3386–91.
[18] Sato YS, Yamanoi H, Kokawa H, Furuhara T. Microstructural evolution of ultrahigh carbon steel during friction stir welding. Scr Mater 2007;57:557–60.
[19] Ghosh M, Bhanumurthy K, Kale GB, Krishna J, Chatterjee S. Diffusion bonding of titanium to 304 stainless steel. J Nucl Mater 2003;322:235–41.
[20] Kundu S, Chatterjee S. Diffusion bonding between commercially pure titanium and micro-duplex stainless steel. Mater Sci Eng A 2008;480:316–22.
[21] Lee WB, Schmuecker M, Mercardo UA, Biallas G, Jung SB. Interfacial reaction in steel–aluminum joints made by friction stir welding. Scr Mater 2006;55:355–8.
[22] Fonda RW, Knipling KE. Texture development in the stir zone of near-α titanium friction stir welds. Scr Mater 2009;60:1097–100.
[23] Dressler U, Biallas G, Mercado UA. Friction stir welding of titanium alloy TiAl6V4 to aluminium alloy AA2024–T3. Mater Sci Eng A 2009;526:113–7.
[24] Chen YC, Nakata K. Microstructural characterization and mechanical properties in friction stir welding of aluminum and titanium dissimilar alloys. Mater Des 2009;30:469–74.